Published in final edited form as:
Am J Transplant. 2014 January ; 14(1): 59–69. doi:10.1111/ajt.12526.

Costimulation blockade alters germinal center responses and prevents antibody-mediated rejection

Eugenia J Kim[1,*], **Jean Kwun**[1,*], **Adriana C Gibby**[1], **Jung Joo Hong**[2,3], **Alton B Farris III**[2], **Neal N Iwakoshi**[1], **Francois Villinger**[2,3], **Allan D Kirk**[1], and **Stuart J Knechtle**[1,†]

[1]Emory Transplant Center, Department of Surgery, Emory University School of Medicine, Atlanta, GA 30322

[2]Department of Pathology, Emory University School of Medicine, Atlanta, GA 30322

[3]Yerkes National Primate Research Center, Emory University, Atlanta, GA 30322

Abstract

De novo donor-specific antibody (DSA) after organ transplantation promotes antibody-mediated rejection (AMR) and causes late graft loss. Previously, we demonstrated that depletion using anti-CD3 immunotoxin (IT) combined with tacrolimus and alefacept (AMR regimen) reliably induced early DSA production with AMR in a nonhuman primate kidney transplant model. Five animals were assigned as positive AMR controls, four received additional belatacept, and four received additional anti-CD40 mAb (2C10R4R4). Notably, production of early de novo DSA was completely attenuated with additional belatacept or 2C10R4R4 treatment. In accordance with this, while positive controls experienced a decrease in peripheral IgM^+ B cells, bela- and 2C10R4-added groups maintained a predominant population of IgM^+ B cells, potentially indicating decreased isotype switching. Central memory T cells ($CD4^+CD28^+CD95^+$) as well as $PD1^{hi}CD4^+$ T cells were decreased in both bela-added and 2C10R4-added groups. In analyzing germinal center (GC) reactions in situ, lymph nodes further revealed a reduction of B cell clonal expansion, GC-Tfh cells, and IL-21 production inside germinal centers with additional belatacept or 2C10R4 treatment. Here we provide evidence that belatacept and 2C10R4 selectively suppresses the humoral response via regulating follicular helper T cells and prevents AMR in this non-human primate model.

Address correspondence to: Stuart J. Knechtle, Emory Transplant Center, 101 Woodruff Circle, WMB 5105, Atlanta, GA 30322, USA. Phone: 404.712.9910; Fax: 404.727.3660; stuart.knechtle@emoryhealthcare.com.
*EJK and JK have equally contributed and appeared in alphabetical order.

Disclosures
The authors of this manuscript have no conflicts of interest to disclose

Author Contributions
E.J.P. designed experiments, performed surgical procedures and cared for experimental macaques, conducted in vitro experiments, interpreted data and prepared the manuscript.
J.K. designed experiments, performed surgical procedures, cared for experimental macaques, conducted in vitro experiments, interpreted data and prepared the manuscript.
A.C.G. conducted in vitro experiments.
J.H. performed histology and immunohistochemistry, interpreted data and prepared the manuscript.
A.B.F. interpreted data (pathologist
N.N.I. interpreted data and prepared the manuscript
F.V. interpreted data and prepared the manuscript
A.D.K. interpreted data and prepared the manuscript
S.J.K. conceived of experimental design, performed surgical procedures, cared for experimental macaques, interpreted data and prepared manuscript.

Keywords

costimulation blockade; antibody-mediated rejection; germinal center reaction; follicular helper T cells

Introduction

In the last decade, donor-specific anti-HLA antibodies (DSA) arising after kidney transplantation, or *de novo* DSA, have been increasingly recognized as a significant cause of late graft loss (1, 2). Specifically, approximately 15–30% of renal transplant recipients develop *de novo* DSA (3, 4), and despite numerous treatment strategies augmenting conventional immunosuppression or targeting the inhibition or removal of B cells, plasma cells, antibodies, and/or complement, no satisfactory therapy has been shown to reliably reverse the effects of DSA once established (5).

While reversal of DSA, or desensitization, has proven to be difficult, several approaches have been successful at preventing antibody formation and antibody-mediated rejection (AMR) after transplantation (6, 7). Among these approaches, the use of costimulation blockade (CoB) to inhibit T-dependent antibody production has been well documented. Larsen et al. demonstrated enhanced inhibition of anti-sheep red blood cell antibodies with LEA29Y (Belatacept, Bristol Myers Squibb) compared to its parent CTLA-4 Ig (8). Lowe et al. (9) observed that blockade of the CD40/40L pathway using anti-CD40 2C10R4 completely blocked antigen-specific antibody production in macaques immunized with keyhole limpet hemocyanin (KLH) antigen. Combined blockade of both CD28:B7 and CD40:40L pathways suppressed DSA formation in kidney-transplanted macaques (10). Belatacept in clinical kidney transplant trials also has been associated with remarkably little DSA (11). The mechanisms of DSA inhibition by CoB, however, have not been fully elucidated.

The above studies highlight the requirement of T cell help for humoral responses after transplantation (12, 13), as $CD4^+$ T cell help is necessary for producing long-lasting IgG isotype-switched alloantibodies (14, 15). In secondary lymphoid organs, T cells primed by antigen presenting cells differentiate into T cell subsets, including the recently defined follicular helper T cell (Tfh cells). Tfh cells subsequently migrate into germinal centers (GC) and interface with GC B cells through a number of surface signaling molecules: CD40-40L, CD28-CD80/86, SAP-signaling lymphocyte activation molecule (SLAM, or CD150) family receptors, ICOS-ICOSL, OX40-OX40L, CXCR5-CXCL13, IL-4 and IL-21 receptors, and more (16), resulting in GC B cell differentiation into memory B cells and plasma cells. For both T cell priming by APCs and GC interactions between Tfh cells and B cells, costimulation via the CD28 and CD40 pathways play a critical role and have immediate therapeutic potential (17, 18). We suspect that blockade of these costimulation pathways will prevent effective GC reactions and the consequent production of class-switched DSA.

We therefore investigated the effects of B7-specific belatacept and CD40-specific 2C10R4 on DSA production and resultant antibody-mediated injury to renal allografts in a preclinical model of *de novo* DSA formation. We recently observed that by depleting T cells with an anti-CD3 immunotoxin (A-dmDT390-scfbDb(C207)) and treating with the calcineurin inhibitor tacrolimus and the CD2-specific fusion protein alefacept (LFA3-Ig) during repopulation, treated animals exhibited a mean survival time of 59 days; however, they developed DSA by 4 weeks after transplantation and renal allografts demonstrated morphologic changes characteristic of antibody-mediated injury, namely transplant

glomerulopathy, peritubular capillaritis, and basement membrane thickening and duplication (19). Here, by adding CoB agents to the AMR inducing regimen, we examine the effects on de novo DSA formation and explore the specific effects on Tfh differentiation and function, GC reaction, and the downstream humoral response.

Methods

Animal selection and transplantation

Many of the materials and methods used in this study have been previously outlined in Page et al (19). Male rhesus macaques weighing 4–7kg were tested specific pathogen free and selected for expression of FN18 epitope, the binding site of anti-CD3 immunotoxin (IT). Donor-recipient pairs were selected based on avoidance of MHC class I matches (6 alleles tested), and class II maximal mismatch among available animals. Each animal underwent native nephrectomy and recipient transplantation. All medications and procedures were approved by the Emory University Institutional Animal Care and Use Committee, and were conducted in accordance with Yerkes National Primate Research Center and the National Institutes of Health guidelines.

Immunosuppression agents

AMR regimen—All animals received the base regimen of anti-CD3 immunotoxin (A-dmDT390-scfbDb(C207), 0.025mg/kg IV twice daily, Massachusetts General Hospital – Dana Farber-Harvard Cancer Center Recombinant Protein Expression and Purification Core Facility, Boston, MA), tacrolimus (Astellas Pharma US, Inc., Deerfield, IL), and alefacept (LFA3-Ig, Astellas Pharma US, Inc., Deerfield, IL). As the original dose of IT given from POD 0–3 produced significant viremia and weight loss, we reduced the immunotoxin dose to 0.025mg/kg IV twice daily on POD 0 and 1 for the following monkeys: DP7D, FA5K, FA5N, DR6G, DW11, and RDk12. To alleviate potential symptoms of cytokine storm, methylprednisolone 125mg was injected intravenously on days the animals received IT. Tacrolimus was started at 0.05mg/kg intramuscular injection twice daily on the day of transplantation, and titrated through day 180 to maintain a trough of 8–12ng/mL. Alefacept was administered at 0.3mg/kg once weekly for 8 weeks, starting on POD −3, 0, then 7, 14, etc, based on the dosage used in Weaver et al (20). Rescue immunosuppression with methylprednisolone (40, 62.5 or 125mg) IM or IV for 3 days was used when the animal exhibited signs of acute rejection or with reduced tacrolimus administration due to weight loss (Figure 1)

Study groups—Five animals were assigned to the AMR positive control arm of IT + tacrolimus + alefacept alone, four of which have been previously reported (19). Four animals were assigned to receive 20mg/kg IV of LEA29Y (belatacept, Bristol-Myers Squibb, Princeton, NJ) on post-transplant days −3, 0, 3, 7, 14, 28, 42, and 56, in addition to the base AMR regimen. Four animals were assigned to receive 20mg/kg IV of the chimeric mouse-rhesus IgG4 anti-CD40, 2C10R4 (REF) (Nonhuman Primate Reagent Resource, Boston, MA) on post-transplant days 0, 7, 14, 28, 42, and 56, in addition to the base AMR regimen.

Allograft and immune monitoring

Peripheral blood was obtained weekly by femoral venipuncture for allograft and immune monitoring. Peripheral blood mononuclear cells (PBMCs) were isolated by Ficoll method using 5mL of lymphocyte separation medium (Mediatech, Inc, Manassas, VA) per sample. Washed PBMCs were surface stained with the following antibodies: Alexa-Fluor 700 or PerCP Cy5.5 conjugated anti-CD3 (SP34-2), PerCP-Cy5.5 conjugated anti-CD4 (L200), APC-Cy7 or Pacific Blue conjugated anti-CD8 (RPA-T8) and Alexa Fluor ®700 conjugated

IgG (G18–145) (all from BD Pharmingen, San Diego, CA); PE-Cy7 conjugated anti-CD28 (CD28.2), eFluor450 conjugated anti-CD95 (DX2) and APC conjugated anti-human CD279 (J105) (All from Ebioscience, San Diego, CA); APC-Cy7 conjugated CD20 (2H7) and Pacific Blue conjugated IgM (MHM-88) (Both from Biolegend, San Diego, CA). FITC conjugated Goat anti-human IgD (δ chain specific, catalog no.2030-02) was obtained from Southern Biotech (Birmingham, AL). PE conjugated CXCR5 (710D82.1) from Nonhuman Primate Reagent Resources (Boston, MA) and PE conjugated Anti-human CXCR5 (MU5UBEE; only for figure 5b) from eBioscience (San diego, CA) were used for Tfh cell staining. Cells were then processed to detect Ki-67 using intracellular staining with Fix/Perm solution (Ebioscience) and PE conjugated anti-Ki-67 (BD Pharmingen, San Diego, CA). Lymph node tissues were crushed through a 100μm strainer, washed, and stained with the above antibodies. Samples were collected with an LSRII flow cytometer (BD Biosciences, San Jose, CA) and analyzed using FlowJo software 9.2. (Tree Star, Ashland, OR

Detection of donor specific antibodies

Alloantibody production was retrospectively assessed by flow cytometric crossmatch of donor PBMCs with serially collected recipient serum samples. Donor PBMCs were coated with ChromPure goat IgG (Jackson ImmunoResearch, West Grove, PA) and incubated with recipient serum. Cells were stained with FITC-labeled anti-monkey IgG (KPL, Inc. Gaithersburg, MD), PE CD20 (BD Pharmingen), and PerCP CD3 (BD Pharmingen). A two-fold increase in mean fluorescence intensity from pre-transplant values was used to define alloantibody positivity, with all positive shifts being greater than 100 shift in mean fluorescence intensity.

Histology, immunofluorescence staining, and quantitative image analysis

Renal allograft tissues were obtained at time of rejection or sacrifice, fixed in 10% neutral buffered formalin, and embedded in paraffin. Embedded tissue blocks were sliced into five-micron-thick sections, deparaffinized in xylene, and rehydrated through graded ethanol to water for H&E and PAS stains as well as immunohistochemical analysis. For germinal center and Tfh cell staining, LN biopsies were fixed by immersion in neutral-buffered 10% formalin and embedded in paraffin. Immunofluorescence staining was performed for CD4, CD20, CD3, Ki67, IL-21 and PD-1 to identify the GC in lymph nodes, as previously described (21). In brief, 4 to 5 μm tissue sections deparaffinized and rehydrated. Heat-induced epitope retrieval were performed with DIVA Decloaker and then blocked with the SNIPER reagent (Biocare, Walnut Creek, CA) for 15 min and in PBS/0.1% triton-X100/4% donkey serum for 30 min at room temperature. Subsequently, the sections were incubated with goat anti-human PD-1 (R&D system, Minneapolis, MN), mouse anti-human Ki67 (clone MM1, Vector, Burlingame, CA), rabbit or mouse anti-human CD20 (Thermo scientific, Rockford, IL or clone L26, Novocastra Laboratories, UK), mouse anti-human CD4 (clone BC/1F6, Abcam, Cambridge, MA), rabbit polyclonal anti-human IL-21 (AbD serotec, Raleigh, NC) and rat anti-human CD3 (clone CD3-12, AbD serotec, Raleigh, NC) antibodies diluted 1:20 to 1:100 in blocking buffer for 1h at room temperature. Thereafter, the sections were incubated with secondary antibodies (Alexa fluor 488/Cy3/Cy5 conjugated appropriate donkey anti-mouse/rabbit/rat/goat antibodies) diluted 1:1000 (Jackson ImmunoResearch, West Grove, PA) in blocking buffer for 30 min at room temperature. Finally, the sections were stained with Hoechst 33342 (Invitrogen, Carlsbad, CA) diluted in water to 0.0025% for 10 min at room temperature, rinsed again, and mounted in warmed glycerol gelatin (Sigma, St Louis, MO) containing 4 mg/ml n-propyl gallate (Fluka, Switzerland). Between each step, the sections were washed three times with blocking buffer. All images were acquired with an Axio Imager Z1 microscope (Zeiss) using various objectives. For quantification, the stained area was calculated using AxioVs40 V4.8.1.0

program (Zeiss). Positive fluorescence signals of Ki67 and IL-21 within follicles were measured using Image J1.43u (NIH). Labeled cells (PD-1^+ $CD4^+$ cells) were be manually counted using FluoView software 1.7 (Olympus). Transplant pathologists reviewed all histology and immunohistochemistry in a blinded fashion.

Statistics

Experimental variables were analyzed by Prism statistical analysis program (GraphPad Software 6.0, San Diego, CA) or SPSS 19 (IBM, Chicago, IL) using the log-rank test for differences in graft survival and nonparametric Mann-Whitney or Kolmogorov-Smirnov tests for others. When box-and whiskers plots are used, the box size represents the limits of the data for the second and third quartiles, with median shown as a bar. The whiskers define the minimum and maximum of the data represented. Error bars represent the mean ± SD in all bar graphs. Values of p less than 0.05 were considered to be statistically significant.

Results

The effect of additional costimulation blockade on de novo antibody-mediated rejection model

All rhesus macaques received the AMR regimen of CD3 immunotoxin, alefacept, and tacrolimus maintenance, as outlined in the methods. Five animals were assigned as positive AMR controls, four of which were previously reported (19). Four animals received additional belatacept and four received additional 2C10R4. While the five AMR control animals (n=5) were sacrificed for graft rejection (MST= 59.4 days), seven of eight animals receiving additional CoB were sacrificed due to poor clinical condition reached the end-point IACUC criteria (weight loss greater than 25%) or per recommendation of attending Yerkes veterinarian (weight loss less than 25% with poor prognosis) but not due to allograft rejection (MST = 54.8 days). Sacrifice time points were similar in all three groups (n=0.632), allowing for comparable analysis of organs (i.e. blood, lymph nodes, spleens, allografts) procured at time of sacrifice. One animal (RDk12) from additional 2C10R4 treated group was sacrificed at day 179 for bladder outlet obstruction caused by bladder stone. Dosing strategy, clinical intervention, reasons for euthanasia are summarized in figure 1. Serum creatinine (sCr) level at the time of sacrifice was significantly lower in additional CoB treated groups compared to AMR controls (0.95±0.27 vs. 5.74±2.17; $p<0.001$). The data suggest that additional costimulation blockade alleviates early graft rejection in this T cell depletion-induced non-human primate AMR model

Costimulation blockade suppresses early de novo DSA production shown in an antibody-mediated rejection-inducing regimen

The addition of CoB showed dramatic improvement in preventing allograft rejection based on longitudinal evaluation of sCr levels (Figure 2a). As described previously, the AMR regimen-treated animals showed varying degrees of transplant glomerulopathy, arteriolar endothelial injury and C4d deposition (19). However, explanted grafts revealed a decrease in cellular rejection and antibody-mediated transplant glomerulopathy in belatacept- and 2C10R4-treated animals (Figure 2b). While AMR controls demonstrated glomerular basement membrane thickening and striation on electron microscopy, a hallmark of antibody-mediated injury, both CoB treatments prevented this process (Figure 2c). Notably, production of early de novo DSA was completely attenuated for both CoB-treated groups at 4 and 6 weeks post transplantation compared to AMR positive controls (Figure 2d). These data suggest that in this depletion-based AMR model, additional CoB suppresses de novo DSA production and antibody-mediated injury.

Costimulation blockade prevents the maturation of B cells in peripheral blood and memory T cell populations in secondary lymphoid organs

All animals exhibited an initial drop in peripheral blood B cells, as previously observed (19); AMR controls increased their peripheral counts back to baseline by one month after transplantation, but animals treated with CoB suppressed this repopulation (Figure 3a). Compared to AMR controls, CoB treated animals had fewer memory-phenotype B cells ($CD27^+CD20^+$) and a predominance of IgM^+ B cells by day 28 (Figure 3b). Consistent with this finding, CoB-treated animals had reduced proliferation of class switched IgG^+ B cells in peripheral blood (Supplemental figure 1). These data suggest that CoB suppresses B cell differentiation to memory and isotype switching – and thus maintains a more naïve phenotype of remaining circulating B cells.

All animals had sustained peripheral T cell depletion after transplantation (Figure 3c). Consistent with previous report, rapid phenotypic switching from naïve to memory T cells was observed in AMR controls. However, both CoB-treated groups showed decreased percentages of central memory T cells (Tcm, $CD4^+CD28^+CD95^+$) compared to the AMR controls and maintained percentages of naïve T cells ($CD4^+CD28^+CD95^-$) compared to the healthy controls, particularly in secondary lymphoid organs (Figure 3d), which likely reflects the requirement of costimulation for T cell differentiation after priming by APC. Additionally, Tfh cells have been speculated to differentiate into the Tcm phenotype (22), and this bulk decrease in Tcm could be surmised to have decreased T cell help for B cell activation.

Costimulation blockade suppresses GC reconstruction after T cell depletion

Since the GCs are the sites for clonal B cell expansion, affinity maturation, and isotype switching (23), we evaluated GC development within lymph nodes. We previously reported that T cells, even with profound depletion, were not completely depleted from the lymph nodes compared to those in blood, spleen and bone marrow (19). Interestingly, despite incomplete depleting T cells, CD3-immunotoxin abolished GC structure in the lymph nodes as well as spleen (Figure 4a). Based on CD20 staining areas, the average B cell follicle size was comparable across all treatment groups as well as in healthy controls (Figure 4b and 4c). This result suggests that the B cell population in lymph nodes are largely unaffected by potent immunosuppression, unlike in peripheral blood. GC size and frequency did not vary significantly between healthy and AMR positive controls, given the heterogeneic GC responses in normal healthy rhesus macaques (Supplemental Figure 2). However, GC frequency and size were dramatically reduced in the belatacept- and 2C10R4-treated groups (Figure 4d and 4e); in contrast, belatacept treatment alone only minimally reduced GC frequency and size (Supplemental Figure 3), as previously shown (24). Since we also observed initial obliteration of GC after T cell depletion, this underscores the effect of combining CoB with T cell depletion, as neither belatacept alone or T cell depletion without CoB (i.e. AMR positive controls) were able to elicit this effect.

PD-1^+CD4 T cells in lymph nodes

Given the role of CD28 and CD40 signaling during T cell differentiation we hypothesized that inhibition of T cell help, especially Tfh cells, may be involved in the decrease in DSA seen in treated animals because highly specialized follicular helper T cells are crucial to GC development (25, 26). We thus evaluated lymph node cells for Tfh phenotypes from tissues procured at necropsy time points. Tfh cells, which tightly regulate the GC reaction, are characterized by high expression of CXCR5, BCL-6, PD-1 and ICOS (27). We confirmed by flow cytometry that PD-1^{hi} CD4 T cells were greatly reduced in CoB-treated recipients (Figure 5a). In contrast, $CXCR5^+$CD4 T cells in the lymph node showed no difference among treatment groups (data not shown). It is difficult, however, to extrapolate these

populations as representing GC-Tfh, given that PD-1 is expressed by other $CD4^+$ T cells (28), and that the nature of $CXCR5^+CD4$ T cells in rhesus macaques is unclear (27). However, flow analysis of LN cells from healthy animal with newly defined antibodies (which was not available during the present study) revealed high level of homogeneous $PD\text{-}1^+$ expression on $CXCR5^+BCL6^+$ CD4 T cells (Figure 5b).

Costimulation blockade suppresses follicular helper T cells and B cell clonal expansion in lymph nodes

GC-Tfh cells are structurally confined within the GC, flow analysis of minced lymph node cells is unable to preserve its locational information. To identify GC-Tfh cells *in situ*, we immunostained the draining lymph nodes to first demarcate the B cell follicles and GCs for structural context. Clonal B cell expansion ($Ki67^+CD20^+$) inside GCs was significantly higher in the AMR positive controls, but suppressed in animals treated with additional CoB (Figure 6a), consistent with the decrease in circulating peripheral blood IgG^+CD20^+ B cells (Supplemental Figure 1). Once the boundaries of the B cell follicles and GCs were established, GC Tfh cells were identified according to their expression of PD-1. GC-Tfh cells ($PD\text{-}1^{hi}CD4^+$) in lymph nodes were significantly decreased in the belatacept-added group compared to AMR control (Figure 6b). Similarly, IL-21 production in follicles, reflecting GC-Tfh function, was greatly reduced in both belatacept- and 2C10R4-added groups (Figure 6c). Furthermore, IL-21 staining within follicle showed a strong correlation with the DSA level ($r=0.87$). IL-21 has been implicated as a key regulator for Tfh cell development. Tfh cells are also known to express high levels of IL-21 which is required for cognate B cell help and GC formation (29). The downstream effect of decreased IL-21 corresponds to the above finding of decreased clonal expansion of B cells with CoB. A less dramatic difference of GC-Tfh cells was noted in 2C10R4 treated monkeys relative to AMR monkeys, which could be due to PD-1 staining signal from other sources outside of GC such as activated CD4 cells (non GC-Tfh). These data suggest that adding CoB affects Tfh cells and their function in T cell depleted animals that otherwise preserve Tfh function, B cell clonal expansion, and DSA production.

Discussion

The inhibition of T-dependent antibody production by CoB has been previously reported, as discussed above, but the mechanisms through which humoral responses are inhibited are less clear. We assessed the blockade of CD28 and CD40 pathways in a rigorous, clinically relevant preclinical model that paralleled our observations from human trials. In our clinical trials, T cell depletion with alemtuzumab (CAMPATH-1H) with rapamycin maintenance has been associated with increased DSA production during repopulation (30), and preliminary evidence suggests that this can be prevented by belatacept (31). In our primate AMR model, we found that rapidly proliferating CD4 memory T cells that were resistant to T cell depletion correlated with early alloantibody production. The current study illustrates that adding CoB to this model decreased CD4 central memory T cell population in spleen and lymph nodes as well as de novo alloantibody production. This decrease likely represents inhibition of T cell activation via antigen presenting cell driven CD28 signal that triggers the naive T cells to become effector T cells in conjunction with TCR signal. Differentiation and survival of Tfh cells are highly dependent on cognate B cell interaction. Costimulatory molecules CD40L, CD28, ICOS, PD-1 and OX40 are involved in antigen specific contact with B cells expressing MHC class II (16). CoB might alter this cognate interface resulting in the diminished GC response, B cell expansion/differentiation, and downstream DSA production. Furthermore, T cell depletion resulted in early eradication of GC, supported by addition of CoB treatment, in contrast to AMR controls that had fully reconstructed, hyperplastic GC. The early effect of T cell depletion on GC suggests that the depletion

process may intimately affect Tfh cells. That GC responses return in the AMR controls also suggests that Tfh cells are specifically inhibited by CoB. The inhibition of GC B cell clonal expansion and Tfh function (with IL-21 expression) required the combination of both CoB and T cell depletion, as belatacept alone did not accomplish this effect.

Neither CoB nor T cell depletion alone was sufficient for producing long-term effects on the germinal center reaction and antibody response. Our clinical experience with T cell depletion using alemtuzumab showed upregulated humoral responses, with increased DSA and serum B cell activating factor (BAFF) levels (32). A significant subset of multiple sclerosis patients treated with alemtuzumab had increased IL-21 levels, which correlated with development of autoimmune thyroiditis (33). Thus, despite extensive T cell depletion, T cells refractory to depletion may continue to provide B cell help. CD28 and CD40 have been known to be required for GC formation, as animals deficient in one or both molecules cannot induce proliferative B cell expansion, class-switch recombination, and GC formation in response to T dependent antigens (34, 35). However, while treatment with CTLA-4Ig (abatacept) suppressed acquisition of Tfh cell phenotype in lymph nodes of a murine rheumatoid arthritis model, clonal expansion of B cells remained intact (36). Also, macaques treated with long-term belatacept were found to have only minimal to moderate reductions in GC size, compared to the profound reduction we observed when combining belatacept with T cell depletion (24). Animals also developed anti-KLH antibodies upon cessation of belatacept, demonstrating the reversible and transient nature of T-dependent antibody inhibition by belatacept alone (24). This implies that targeting Tfh cells by combining T cell depletion with CoB has a more profound and lasting downstream effect on humoral responses, namely the alloantibody response. This is further supported by our long-term surviving monkey, RDk12, who failed to demonstrate DSA at 179 days, well beyond completing an anti-CD40 treatment course on day 56 (Supplemental figure 4). This effect was likely donor-specific and not due to generalized over-immunosuppression, as the animal was able to mount GC reactions comparable to healthy controls at 179 days.

Due to its clinical outcome (poor prognosis/weight loss) and drug availability, the exact regimen is not clinically translatable. While a poor therapeutic agent, the anti-CD3 immunotoxin in combination with tacrolimus and alefacept was efficient at producing DSA and AMR and thus served as a robust preclinical NHP AMR model. Our results show that adding CD28 or CD154 CoB can suppress Tfh cell differentiation, B cell clonal expansion, GC reaction, and DSA formation that conventional immunosuppressants such as tacrolimus fail to prevent in our AMR model. Moreover, the novel finding that COB combined with T cell depletion specifically produces these effects on the B cell has implications for potential clinical use, particularly for the reduction of humoral responses. The data support further testing of costimulation blockade and depletional induction therapy in a clinically translatable regimen to reduce post-transplant humoral response. While risks of over-immunosuppression must be considered, these results support the use of belatacept and CD40 blockade in combination with lymphodepletion to prevent AMR.

Supplementary Material

Refer to Web version on PubMed Central for supplementary material.

Acknowledgments

This work was supported by the NIH 1U01AI074635 awarded to S.J.K., NIH R01AI078775 to F.V. and collaboration with the Yerkes National Primate Center (Yerkes base grant OD P51POD111). We would like gratefully acknowledge; Drs. Andrew Adams and Mandy Ford for critical review of the manuscript; Frank Leopardi and Kelly Hamby for assisting in animal surgeries; the YNPRC staff and the expert assistance of Drs. Elizabeth Strobert and Joe Jenkins for animal care; the Emory Transplant Center Biorepository team for their work in weekly

viral monitoring; and Hong Yi and the Robert P. Apkarian Integrated Electron Microscopy Core of Emory University for their work in tissue analysis for electron microscopy. Reagents used in this study were provided by the Nonhuman Primate Reagent Resource (HHSN272200900037C).

Abbreviations

DSA	donor-specific antibodies
AMR	antibody-mediated rejection
CoB	costimulation blockade
CTLA-4	Cytotoxic T-Lymphocyte Antigen 4
GC	germinal center
Tfh	T follicular helper
SLAM	signaling lymphocyte activation molecule
SAP	SLAM-associated protein
ICOS	inducible T cell costimulator
APC	antigen presenting cell
LFA3	lymphocyte function associated antigen 3
IT	immunotoxin
PBMC	peripheral blood mononuclear cell
PD-1	programmed cell death 1
BAFF	B cell activating factor
Tcm	central memory T cells
KLH	keyhole limpet hemocyanin

References

1. Loupy A, Hill GS, Jordan SC. Nat Rev Nephrol. 2012; 8(6):348–357. [PubMed: 22508180]
2. Terasaki PI. Transplantation. 2012; 93(8):751–756. [PubMed: 22453870]
3. Wiebe C, Gibson IW, Blydt-Hansen TD, Karpinski M, Ho J, Storsley LJ, et al. Am J Transplant. 2012
4. Hidalgo LG, Campbell PM, Sis B, Einecke G, Mengel M, Chang J, et al. Am J Transplant. 2009; 9(11):2532–2541. [PubMed: 19843031]
5. Everly MJ, Terasaki PI. Semin Immunol. 2012; 24(2):143–147. [PubMed: 22153981]
6. Kelishadi SS, Azimzadeh AM, Zhang T, Stoddard T, Welty E, Avon C, et al. Preemptive CD20+ B cell depletion attenuates cardiac allograft vasculopathy in cyclosporine-treated monkeys. The Journal of clinical investigation. 2010; 120(4):1275–1284. [PubMed: 20335656]
7. Wang H, Arp J, Liu W, Faas SJ, Jiang J, Gies DR, et al. Inhibition of terminal complement components in presensitized transplant recipients prevents antibody-mediated rejection leading to long-term graft survival and accommodation. Journal of immunology. 2007; 179(7):4451–4463.
8. Larsen CP, Pearson TC, Adams AB, Tso P, Shirasugi N, Strobert E, et al. Rational development of LEA29Y (belatacept), a high-affinity variant of CTLA4-Ig with potent immunosuppressive properties. Am J Transplant. 2005; 5(3):443–453. [PubMed: 15707398]
9. Lowe M, Badell IR, Thompson P, Martin B, Leopardi F, Strobert E, et al. Am J Transplant. 2012; 12(8):2079–2087. [PubMed: 22845909]
10. Pearson TC, Trambley J, Odom K, Anderson DC, Cowan S, Bray R, et al. Anti-CD40 therapy extends renal allograft survival in rhesus macaques. Transplantation. 2002; 74(7):933–940. [PubMed: 12394833]

11. Vincenti F, Larsen CP, Alberu J, Bresnahan B, Garcia VD, Kothari J, et al. Three-year outcomes from BENEFIT, a randomized, active-controlled, parallel-group study in adult kidney transplant recipients. Am J Transplant. 2012; 12(1):210–217. [PubMed: 21992533]
12. Parker DC. T cell-dependent B cell activation. Annu Rev Immunol. 1993; 11:331–360. [PubMed: 8476565]
13. Lenschow DJ, Walunas TL, Bluestone JA. CD28/B7 system of T cell costimulation. Annu Rev Immunol. 1996; 14:233–258. [PubMed: 8717514]
14. Steele DJ, Laufer TM, Smiley ST, Ando Y, Grusby MJ, Glimcher LH, et al. Two levels of help for B cell alloantibody production. The Journal of experimental medicine. 1996; 183(2):699–703. [PubMed: 8627185]
15. Conlon TM, Saeb-Parsy K, Cole JL, Motallebzadeh R, Qureshi MS, Rehakova S, et al. Germinal center alloantibody responses are mediated exclusively by indirect-pathway CD4 T follicular helper cells. Journal of immunology. 2012; 188(6):2643–2652.
16. Crotty S. Follicular helper CD4 T cells (TFH) . Annu Rev Immunol. 2011; 29:621–663. [PubMed: 21314428]
17. Nonoyama S, Hollenbaugh D, Aruffo A, Ledbetter JA, Ochs HD. B cell activation via CD40 is required for specific antibody production by antigen-stimulated human B cells. The Journal of experimental medicine. 1993; 178(3):1097–1102. [PubMed: 7688786]
18. Klaus SJ, Pinchuk LM, Ochs HD, Law CL, Fanslow WC, Armitage RJ, et al. Costimulation through CD28 enhances T cell-dependent B cell activation via CD40-CD40L interaction. Journal of immunology. 1994; 152(12):5643–5652.
19. Page EK, Page AJ, Kwun J, Gibby AC, Leopardi F, Jenkins JB, et al. Enhanced De Novo Alloantibody and Antibody-Mediated Injury in Rhesus Macaques. Am J Transplant. 2012
20. Weaver TA, Charafeddine AH, Agarwal A, Turner AP, Russell M, Leopardi FV, et al. Alefacept promotes co-stimulation blockade based allograft survival in nonhuman primates. Nat Med. 2009; 15(7):746–749. [PubMed: 19584865]
21. Hong JJ, Amancha PK, Rogers K, Ansari AA, Villinger F. Spatial alterations between CD4(+) T follicular helper, B, and CD8(+) T cells during simian immunodeficiency virus infection: T/B cell homeostasis, activation, and potential mechanism for viral escape. Journal of immunology. 2012; 188(7):3247–3256.
22. Pepper M, Jenkins MK. Nature immunology. 2011; 12(6):467–471. [PubMed: 21739668]
23. MacLennan IC. Germinal centers. Annu Rev Immunol. 1994; 12:117–139. [PubMed: 8011279]
24. Haggerty HG, Proctor SJ. Toxicological sciences : an official journal of the Society of Toxicology. 2012; 127(1):159–168. [PubMed: 22331490]
25. McHeyzer-Williams LJ, Pelletier N, Mark L, Fazilleau N, McHeyzer-Williams MG. Follicular helper T cells as cognate regulators of B cell immunity. Curr Opin Immunol. 2009; 21(3):266–273. [PubMed: 19502021]
26. King C. New insights into the differentiation and function of T follicular helper cells. Nat Rev Immunol. 2009; 9(11):757–766. [PubMed: 19855402]
27. Petrovas C, Yamamoto T, Gerner MY, Boswell KL, Wloka K, Smith EC, et al. The Journal of clinical investigation. 2012
28. Day CL, Kaufmann DE, Kiepiela P, Brown JA, Moodley ES, Reddy S, et al. PD-1 expression on HIV-specific T cells is associated with T-cell exhaustion and disease progression. Nature. 2006; 443(7109):350–354. [PubMed: 16921384]
29. Silver JS, Hunter CA. Immunity. 2008; 29(1):7–9. [PubMed: 18631451]
30. Knechtle SJ, Pirsch JD, H Fechner JJ, Becker BN, Friedl A, Colvin RB, et al. Campath-1H induction plus rapamycin monotherapy for renal transplantation: results of a pilot study. Am J Transplant. 2003; 3(6):722–730. [PubMed: 12780564]
31. Kirk AD, Mead S, Xu H, Mehta A, Guasch A, Cheeseman J, et al. Am J Transplant. 2010; 11(s2): 1.
32. Bloom D, Chang Z, Pauly K, Kwun J, Fechner J, Hayes C, et al. BAFF is increased in renal transplant patients following treatment with alemtuzumab. Am J Transplant. 2009; 9(8):1835–1845. [PubMed: 19522878]

33. Jones JL, Phuah CL, Cox AL, Thompson SA, Ban M, Shawcross J, et al. IL-21 drives secondary autoimmunity in patients with multiple sclerosis, following therapeutic lymphocyte depletion with alemtuzumab (Campath-1H) . The Journal of clinical investigation. 2009; 119(7):2052–2061. [PubMed: 19546505]

34. Ferguson SE, Han S, Kelsoe G, Thompson CB. CD28 is required for germinal center formation. Journal of immunology. 1996; 156(12):4576–4581.

35. Kawabe T, Naka T, Yoshida K, Tanaka T, Fujiwara H, Suematsu S, et al. The immune responses in CD40-deficient mice: impaired immunoglobulin class switching and germinal center formation. Immunity. 1994; 1(3):167–178. [PubMed: 7534202]

36. Platt AM, Gibson VB, Patakas A, Benson RA, Nadler SG, Brewer JM, et al. Abatacept limits breach of self-tolerance in a murine model of arthritis via effects on the generation of T follicular helper cells. Journal of immunology. 2010; 185(3):1558–1567.

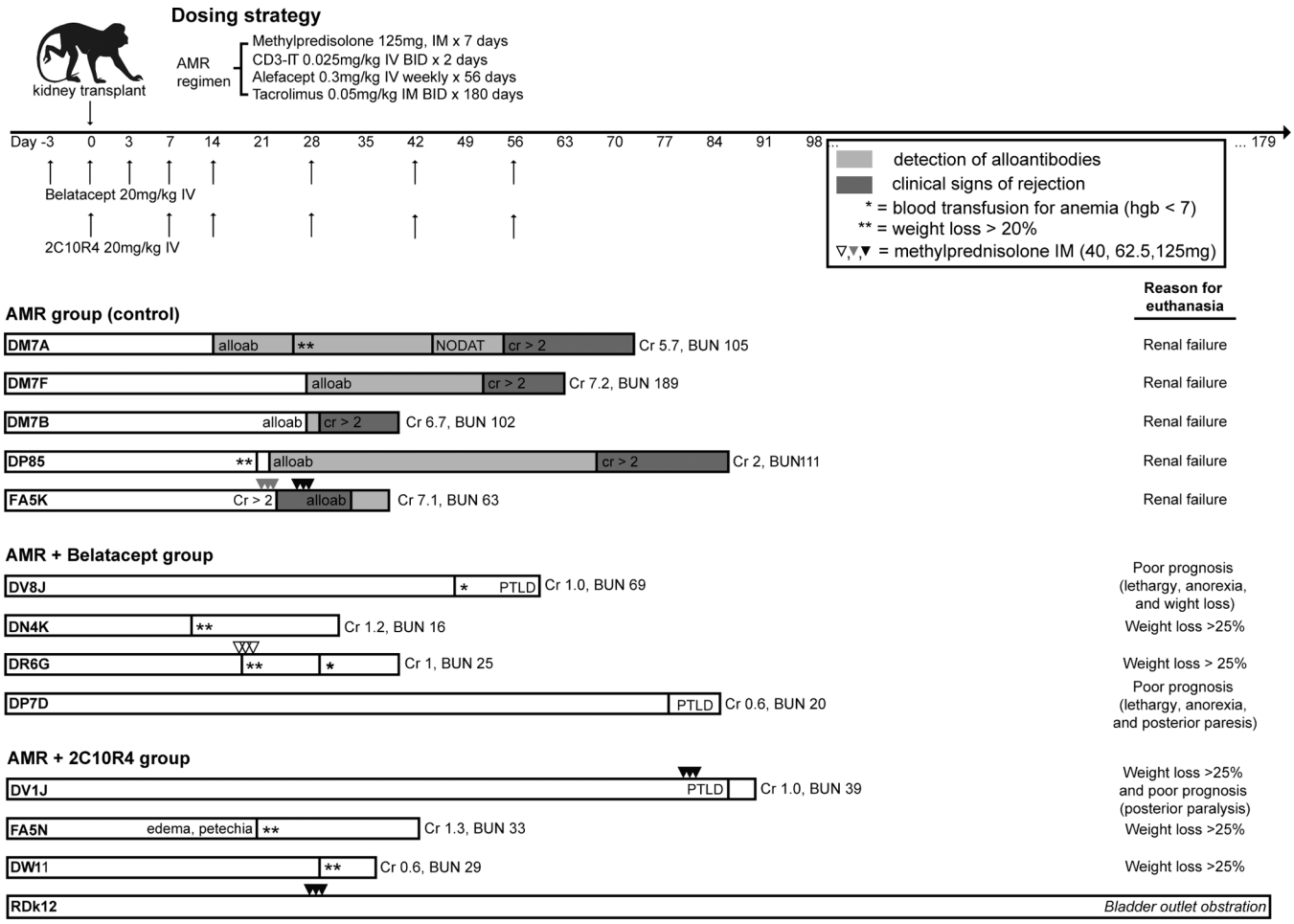

Figure 1. Immunosuppressive regimens, dosing strategy, clinical interventions and outcomes in AMR control and additional costimulation blockade treated rhesus monkeys

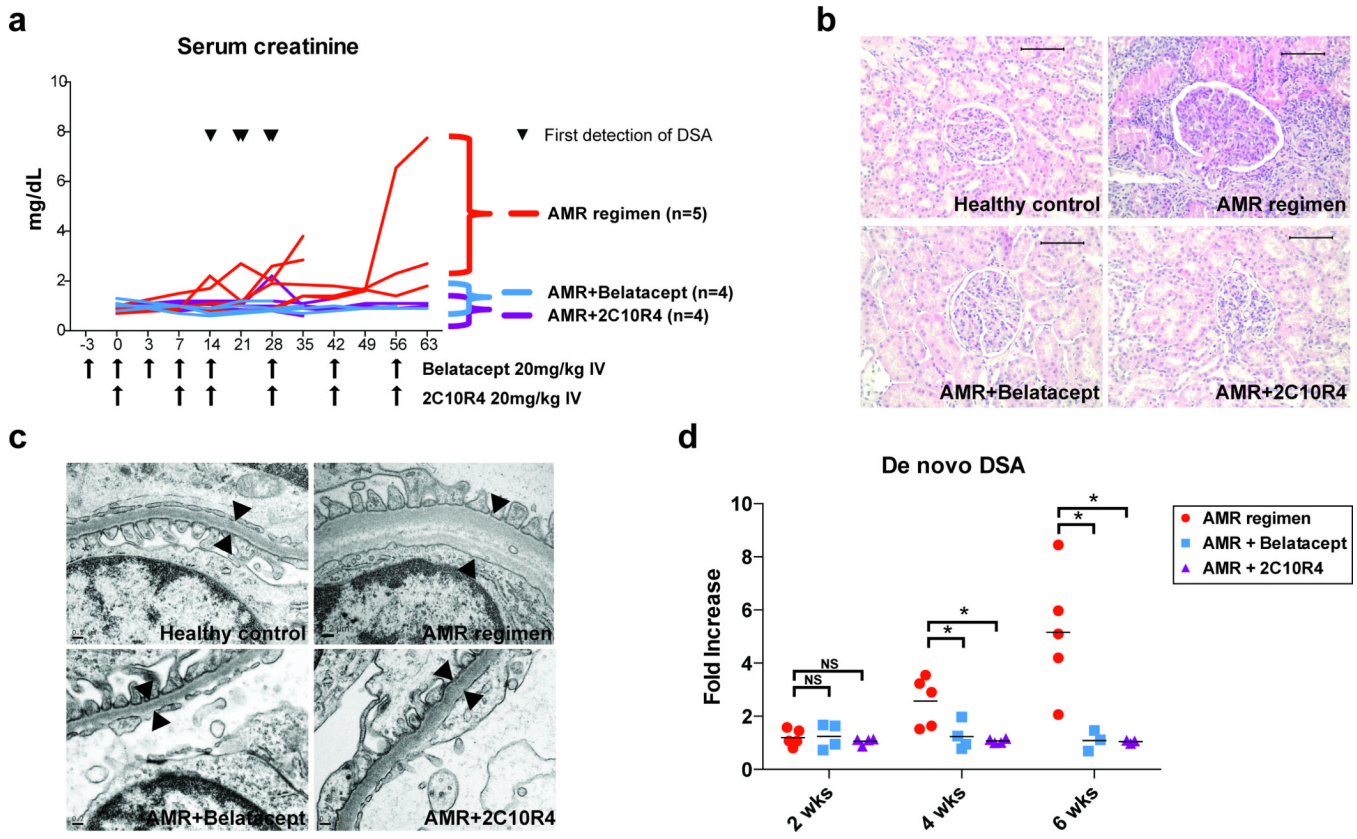

Figure 2. Costimulation blockade prevents allograft rejection and alloantibody production

(a) Serum creatinine level of AMR positive control, belatacept-treated, and 2C10R4-treated groups. AMR positive control group (n=5, red line), receiving CD3-immunotoxin, alefacept, and tacrolimus (trough 8–12ng/mL), had early alloantibody production within 4 weeks from transplantation (the first detection of DSA from AMR positive controls is indicated by ▼) and were sacrificed for graft failure. Belatacept-treated (n=4, blue line) and 2C10R4-treated (n=4, purple line) groups received the AMR regimen plus additional belatacept or additional 2C10R4 for 8 weeks (duration and frequency indicated by arrows along the x-axis); these animals failed to demonstrate DSA production and retained graft function, but were sacrificed for non-rejection end-point criteria. Animal survival was equivalent among the three groups (p=0.632). **(b)** Histological examination of necropsy kidney specimens from healthy control, AMR control, belatacept-added, and 2C10R4-added group. Representative H&E staining portrays evidence of cellular and antibody-mediated rejection in the AMR positive control group, including tubulointerstitial inflammation and transplant glomerulopathy. These features were prevented in animals receiving additional costimulation blockade. Original magnification ×200 (bar scale: 100μm). **(c)** An electron microscopy image of glomerular basement membranes from healthy control, AMR control, Bela-added, and 2C10R4 added group. AMR control animals showed thickening, lamination and duplication of glomerular basement membranes. **(d)** De novo DSA production was inhibited in animals receiving belatacept and 2C10R4. *p<0.05 vs. AMR control.

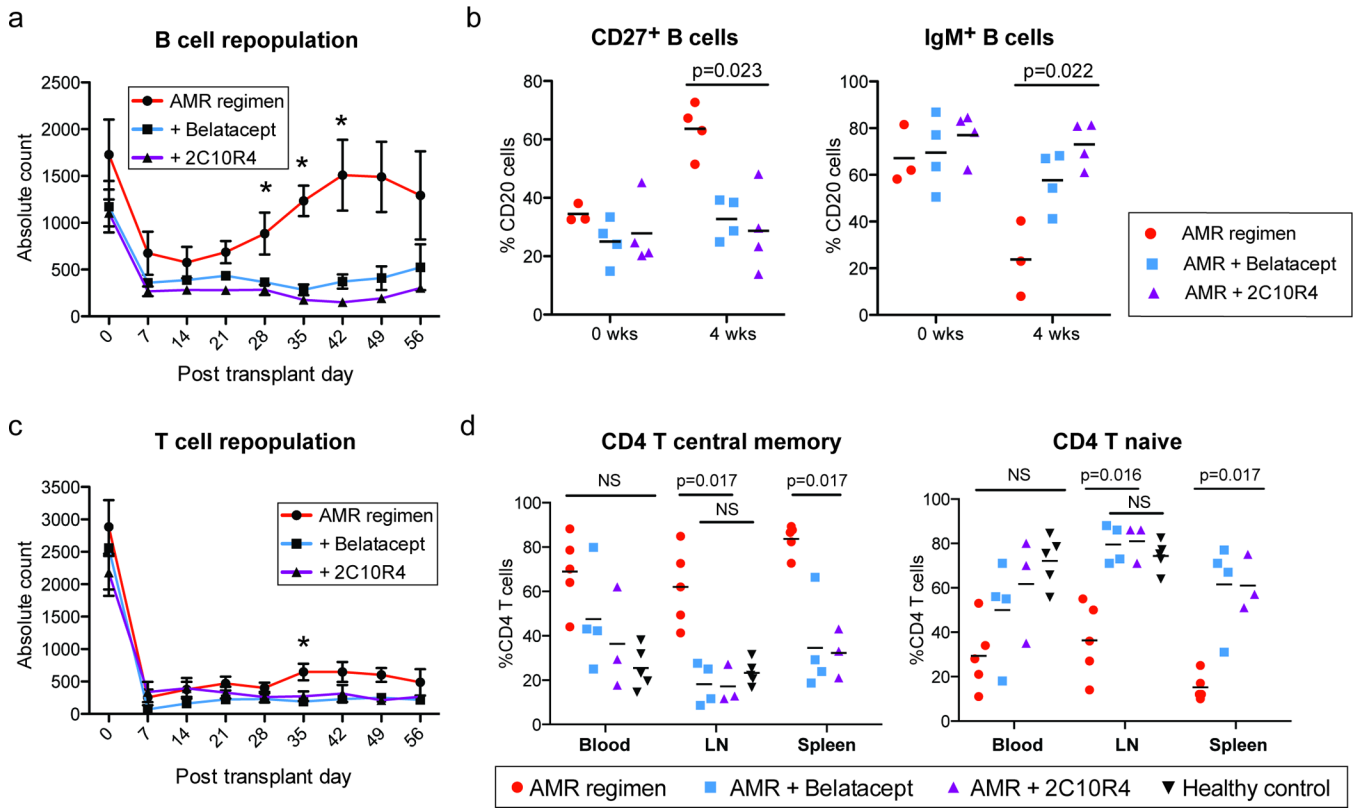

Figure 3. Costimulation blockade prevents B cell repopulation and maturation, and maintains naïve CD4 T cell phenotype in secondary lymphoid organs

(**a**) Peripheral blood B cells decreased after induction immunosuppression, as reported previously [18]. In contrast to AMR controls, CoB treated animals failed to repopulate B cells. *p<0.05 (**b**) Memory type B cells ($CD20^+CD27^+$) are decreased and immature phenotype (IgM^+CD20^+) B cells are predominant in CoB treated animals. The drop in IgM^+ B cells among AMR controls coincides with DSA production and IgG^+B cell proliferation (Supplemental figure 1) **c** Peripheral blood T cells remain decreased in all groups. The isolated difference at 35 days may represent onset of allograft rejection in AMR controls. *p<0.05 (**d** Central memory CD4 T cells ($CD4^+CD28^+CD95^+$) were significantly decreased and CD4 naïve T cells ($CD4^+CD28^+CD95^-$) increased in bela- (n=4, blue) and 2C10R4-added (†n=3, purple) animals in the spleen and inguinal lymph nodes compared to AMR positive controls (n=5, red) at time of necropsy (†One recipient from 2C10R4-added group was censored from this analysis due to its necropsy time point performed at 179d post-transplant; the subject was sacrificed for non-rejection endpoint criteria; supplemental figure 4). NS>0.05.

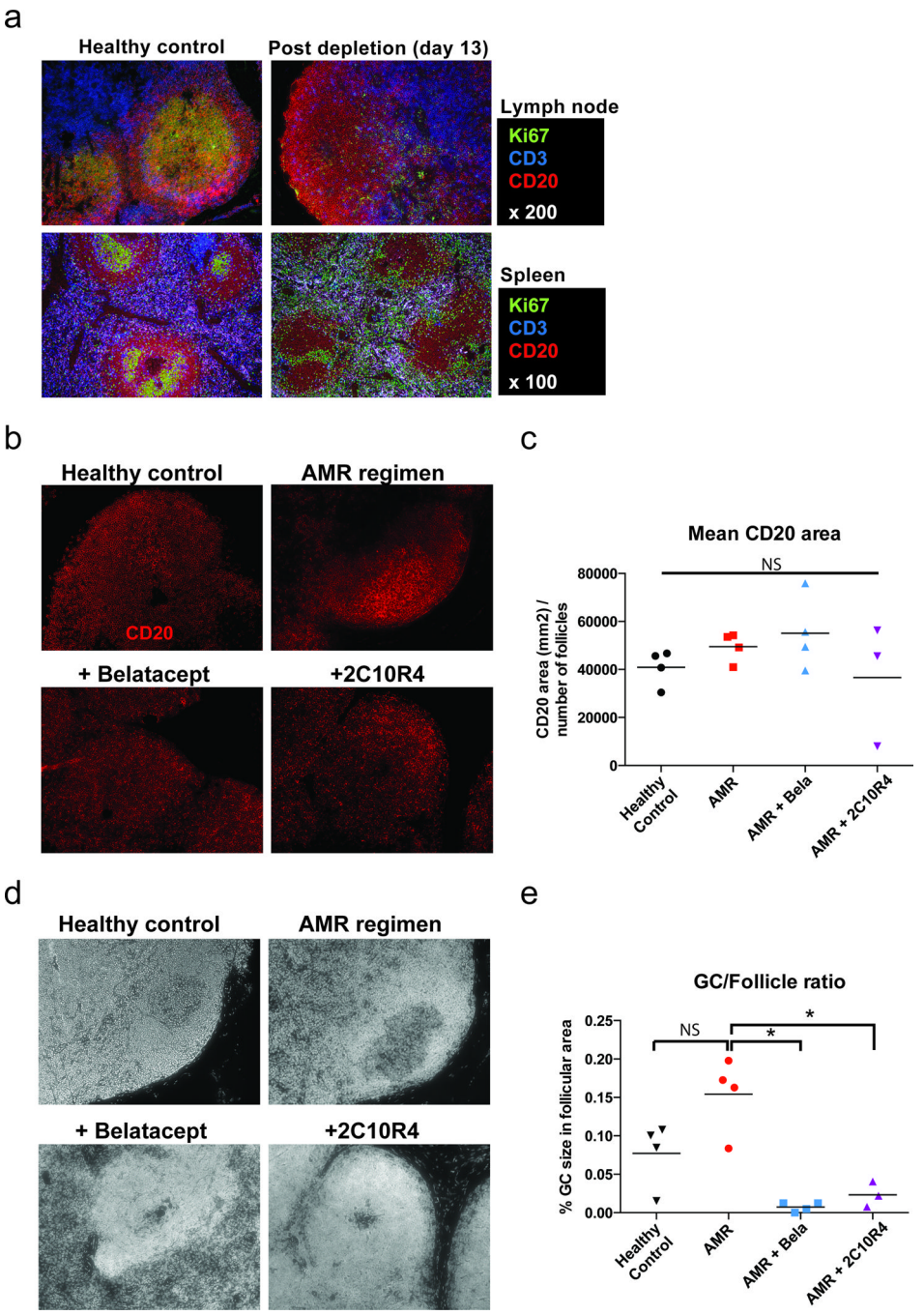

Figure 4. Post-transplant follicle and GC morphology in secondary lymphoid organs

(a) Representative immunofluorescence image of GC staining with CD3 (Blue), CD20 (Red), and Ki67 (Green) in lymph node and spleen sections from untreated (healthy control) and CD3-immunotoxin treated rhesus monkey (post-transplant day 13). **(b)** Immunofluorescence analysis for CD20 (red) staining in lymph node sections from healthy control, AMR positive control, additional belatacept, and additional 2C10R4 treated recipients. Original magnification, ×200. (c) Image J (National Institutes of Health) quantitation of the positive fluorescence signals of CD20 in lymph node sections. Follicle size based on $CD20^{+}$ B cells was similar across all groups, including healthy controls. (d)

Hoechst nuclear staining in paraffin-embedded lymph node sections. Original magnification ×200. GCs in lymph nodes of rhesus macaques were identified by Hoechst nuclear staining. This less intensely stained GC area was confirmed as corresponding to the same area containing proliferating ($Ki67^+$) B cells (Supplemental figure 2). (e) ImageJ quantitation of the less intensely stained Hoechst area. GC size was significantly reduced in Bela- and 2C10R4-added animals compared to AMR positive controls (*$p<0.05$). These data are representative lymph node sections from healthy controls (n=4), AMR positive controls (n=5), Bela-added (n=4), and 2C10R4-added (n=3) rhesus macaque recipients.

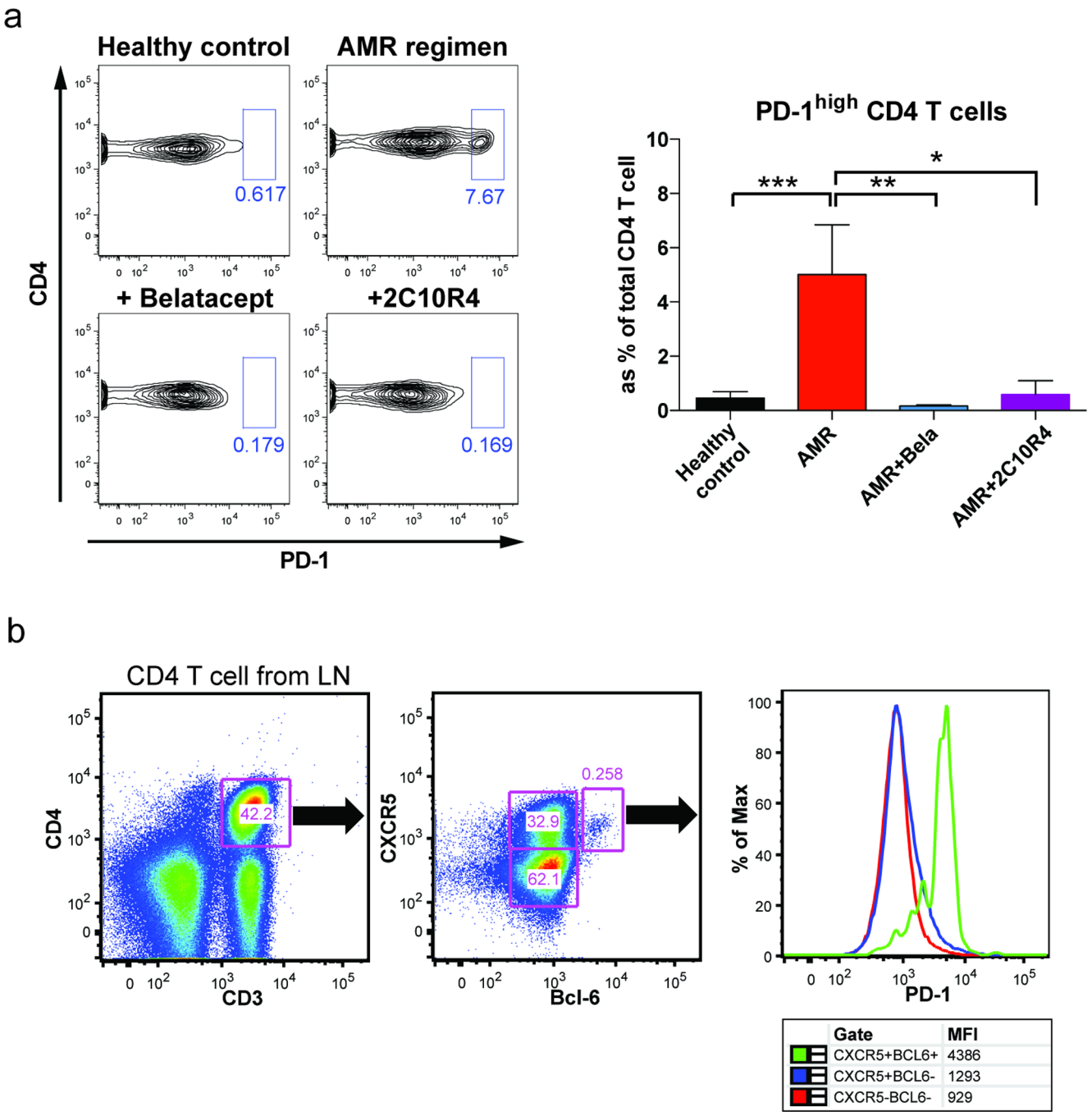

Figure 5. Decreased PD1^{+}CD4^{+} T cells in lymph nodes in additional costimulation blockades treated animals

(a) Flow cytometry contour plots show PD-1 expression among CD4 T cells in draining inguinal lymph nodes from healthy controls (n=5) as well as AMR positive controls (n=5), Bela-added (n=4), 2C10R4-added (n=3) rhesus macaque recipients. The frequency of the gated population (PD-1^{hi}CD4^{+}) is shown as a bar graph. *p<0.05, **p<0.01, ***p<0.001, vs. AMR control. (b) Flow cytometry analysis of CD4 T cells based on the expression of CXCR5 and BCL-6 in the lymph nodes of rhesus macaque. Cells were first gated for CD4 T cells and gated based on the differential expression of CXCR5 and BCL-6. High PD-1

expression was shown in CXCR5^{+}Bcl-6^{+} CD4 T cell subsets. Numbers in dot plots indicate the percentage of cells in each gate.

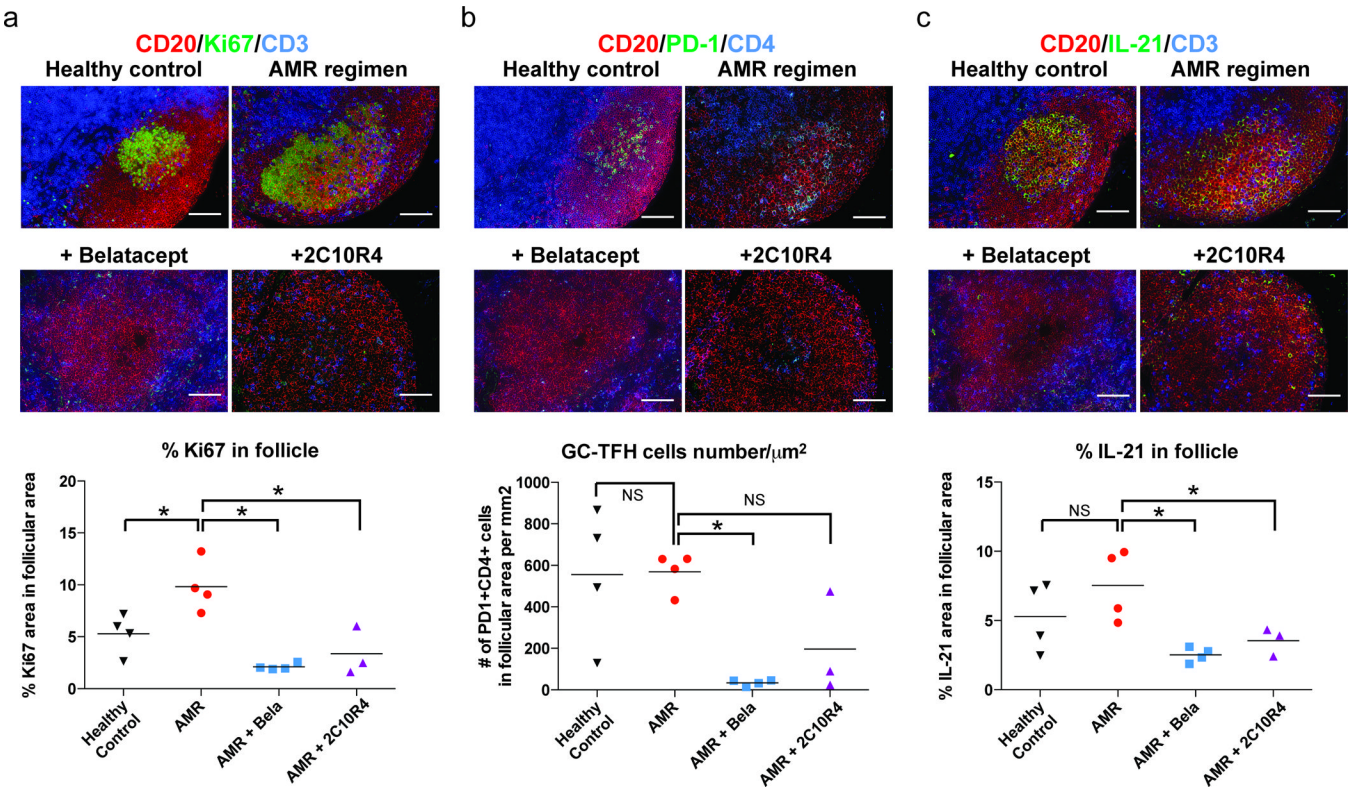

Figure 6. Effects of costimulation blockade on B cell clonal expansion, germinal center-Tfh, and IL-21 production

(a) B cell clonal expansion in germinal centers was significantly increased in AMR group (*p<0.05 vs. healthy control). The increased B cell proliferation found in AMR positive controls was significantly suppressed by additional Belatacept and 2C10R4 (*p<0.05 vs. AMR) treatment. Proliferating B cells in germinal centers are identified by CD20, Ki67 and CD3 staining. **b** Tfh cells were significantly reduced in Bela-added (*p<0.05 vs. AMR) but not in 2C10R4-added (p=0.1429 vs. AMR) rhesus macaques. CD4, CD20, PD-1 were simultaneously analyzed for Tfh cells in the germinal center. **c** IL-21 expression was significantly reduced in Bela-added and 2C10R4-added animals compared to AMR positive controls (*p<0.05). These data are representative lymph node sections from healthy controls (n=4), AMR positive controls (n=5), Bela-added (n=4), and 2C10R4-added (n=3) rhesus macaque recipients. Original magnification ×200 (scale bar: 50μm).